A holistic life cycle design approach to enhance the sustainability of concrete structures

Davide di Summa[1,2], Matteo Parpanesi[2], Liberato Ferrara[2] , Nele De Belie[1].

1. Ghent University, Department of Structural Engineering and Building Materials; Magnel-Vandepitte Laboratory, Tech Lane Ghent Science Park, Campus A, Technologiepark Zwijnaarde 60, B-9052 Ghent, Belgium;
   Davide.diSumma@UGent.be; Nele.DeBelie@UGent.be
2. Politecnico di Milano, Department of Civil and Environmental Engineering, piazza Leonardo da Vinci 32, 20133 Milan, Italy;
   Matteo.Parpanesi@mail.PoliMi.it; Liberato.Ferrara@PoliMi.it

Abstract

The development of innovative cementitious materials such as Ultra High Performance Concrete (UHPC) requires tailored approaches to assess both the environmental and economic impact of structural applications employing them. For this purpose, in this paper, Life Cycle Assessment (LCA) and Life Cycle Cost (LCC) methodologies are integrated into a Durability Assessment-Based Design (DAD) workflow which combines structural design algorithms for UHPC with the assessment of the durability performance, with the aim of predicting the evolution of the structural performance all along the service life (SL) in the intended scenarios. As a case study a water tank made of UHPC has been herein selected and compared to a reference made of Ordinary Reinforced Concrete (ORC). While the ORC solution was designed with cantilever cast in situ walls, two different design concepts were assessed for the UHPC basin: one with cast in situ walls and one with precast slabs supported by ORC columns. Moreover, two different mix designs (mainly differing on the alternative presence of silica fume or slag) have been investigated for the UHPC basin and a SL equal to 50 years has been taken into account for each structure. The optimized design, together with the reduced frequency of the maintenance activities for the UHPC structure, allowed by the UHPC superior material and structural durability, resulted into consistent reductions of environmental impacts, up to 76% as for Human Toxicity and Fresh Water Aquatic Ecotoxicity in comparison to the ORC solution. In addition to this, an assessment of the overall construction and maintenance costs that occur during the lifetime of the structures showed a cost reduction higher than 40% for both UHPC solutions, mainly due to a reduction of up to 6% during the construction phase and 91% for the maintenance activities. This also highlights the importance of the correct metrics in evaluating the sustainability of UHPC structural applications, which has to move forward from the units volume or mass of material and its individual constituents to functional units, representative of the benefits of using advanced cement based materials in structurally and environmentally challenging service scenarios.

Keywords: Holistic sustainability, LCA, LCC, UHPC, Durability Assessed Design

1 Introduction

The Human Right Council of the United Nations recognized, in 2021, globally and for the first time in history, the "human right to a clean, healthy and sustainable environment", followed by a more recent report [1] which better details the risk of the ongoing toxification of people and planet and raises awareness of the ensuing social injustices. More specifically, the report introduces the concept of "sacrifice zones" which are extremely contaminated areas where people, due to the contingent pollution issues, suffer human rights violations as well as physical and mental health consequences. The report also defines the boundaries of the problem which is actually of global interest involving places which include the "Chemical Valley" in Canada and the city of Taranto in Europe, passing through cities like New Delhi in India or Bor in Serbia. Therefore, if on the one hand it clarifies the worldwide need of a more sustainable world (environmentally, economically and socially), on the other hand it forces each production sector to re-think its future to change its current paradigm. In this regard, the construction sector requires a specific attention not only because of its influence on the economy, since it represents around 9% of the EU Gross Domestic Product [2][3] but also because it is estimated to be responsible of the consumption of 50% of the raw materials, of 36% of the global final energy use and of the generation of 25% of the total solid waste worldwide [4][5]. In this framework, concrete is one of the major players whose contribution to the transformation of the construction interest has, as such, aroused a growing scientific interest. This is due to the fact that it is the second most consumed material in the world after water [6] besides the large environmental impacts associated to the production of cement (its main component) which result in 7% of world total CO_2 emissions [7]. Therefore, the industry and academia efforts are focusing not only on the overall sustainability of the production of concrete, including the entire supply chain, but also on the overall

sustainability of the construction sector, considering the entire Service Life (SL) of buildings and structures, until their decommissioning/demolition and treatment of constituent elements and materials as a waste or, alternatively, as recyclable materials and products. In this framework, the concept of material and structural durability has become one of the key factors to address the sustainability issue [8].

As a matter of fact, the inherent and unavoidable cracking of concrete in its structural service conditions, with the ensuing faster ingress of harmful substances inside the bulk of structural elements, accelerates the corrosion process of the steel reinforcement and, in case, the cementitious matrix degradation as well. The consequence is the degradation of the structural performance with the ensuing need to carry out the maintenance activities as soon as the front of the deterioration mechanism reaches a critical depth, e.g. concrete cover depth [9][10]. These maintenance activities, whose frequency may increase after the first one [11], add up to further environmental impact and overall economic burden of the construction sector as a whole. To address the aforesaid problem, innovative cement based materials have been developed which, ensuring the self-repair of the cracks upon occurrence or being extremely impervious to the penetration of harmful substances in aggressive environments, improve the durability of the structure they are built of or retrofitted with [12][13][14][15]. It must be highlighted that the durability represents a design target requisite which in current design codes [16], is achieved through "deemed to satisfy" prescriptions, including minimum water to cement ratio, minimum cement content and minimum concrete cover to guarantee the target service life. Nonetheless, because of the random and sometimes one-of-a-kind characteristics of structural service scenarios, this approach has resulted so far into a continuous need of repairing activities which for ORC structures might represent around 35% of the overall expenses throughout their SL, as already outlined in a previous work for structures exposed to an aggressive chloride environment [8]. Thus, the reiteration of the same design approach will lead to an exacerbation of the sustainability issues of concrete structures both in terms of environmental impact and cost implications throughout their entire SL. Because of this, UHPC started to attract more interest due to its improved durability performance both in the uncracked and cracked state [17][18]. This is due respectively to its low porosity and to the presence of micro-fibres (steel or polymeric) which provide the tensile strain hardening behaviour favoring the formation of small and tightly spaced cracks, tighter than obtainable in ordinary reinforced concrete structures [19][20]. However, its use has been so far somewhat limited by the lack of appropriate design codes [21] and the cost, although Al Obaidi et al. warned about how the cost assessment of UHPC, usually made on the basis on the material cost per unit volume, generates a misperception [22]. This is due to the fact that an estimation as such does not take into consideration the UHPC mechanical and durability properties which allow to conceive, design and build structures using less raw materials while guaranteeing the same structural performance and a longer SL in comparison to a reference ordinary reinforced concrete solution [22]. All the above converges towards the need to employ a design approach able to evaluate the evolution of the structural performance all along the structure service life encompassing the effects of material and structural degradation mechanisms. It is furthermore worth highlighting that for most of the advanced cementitious composites, because of the high cement content and low water to binder ratio, which endows with high compressive strength (generally higher than 100 MPa) and, as said, tensile strain hardening behaviour, deemed to satisfy code specifications for durability are automatically fulfilled.

In the aforesaid framework, this paper investigates the use of a semi-probabilistic approach based on the evaluation over time of structural performance indicators (such as the resistant bending moment), shifting from a "deemed to satisfy" to a Durability Assessment-Based Design (DAD) paradigm. Keeping such point of view, the maintenance activities are quantified and scheduled upon the attainment of a limit state which has to be defined according to the structural service scenario. This conceptual framework is here applied to a real-size case study which is a basin structure aimed to be part of a cooling tower in a geothermal power plant. The structure contains geothermal water rich in chlorides and sulphate ions as in [22] that comes out from the ground during the drilling process and needs to be stored and cooled prior to be re-injected into the soil. LCA and LCC methodologies are used to assess the potential environmental and economical convenience of UHPC in comparison to a conventional reinforced concrete solution considering, as already done in a similar work, as functional unit (FU), a structure built according to the durability and structural specificities of the material which is employed [8][23][24][25] From this point of view, the scope of this research is to carry out a more comprehensive LCA and LCC assessment that, including the analysis of the structural performance throughout the service life, contributes to the validation of a new design approach able to exploit the superior performance of UHPC since the conceptual design phase and not merely in the design check stage. This is in line with the way paved in other studies that highlighted the possibility, for UHPC, to reduce the environmental burdens up to 50% when assessed on a structure scale [25]. The goal is, then, an improvement of the design practice in extremely aggressive scenarios, validating a holistic design approach for innovative cementitious composites capable of favouring, at the same time, their spread to an as broad as possible market.

2 Case study

The structure chosen as a benchmark case study in this paper is a tank intended to serve as geothermal water collector, part of a cooling tower of a geothermal energy plant. Cooling towers work by condensing and transforming in rain the vapour

which is extracted from the subsoil, led to the same tower and then collected in basins. The case here assessed, replicates the layout of a geothermal power plant in Chiusdino (Tuscany, Italy), owned and operated by Enel Green Power and it has been re-designed using both Ordinary Reinforced Concrete (ORC) and UHPC. The geometry and cross sectional dimensions of the existing structure have been used for the ORC structure design, only taking care of the optimization of the reinforcement bars layout. With regard to the UHPC basin, it has been designed keeping the same geometry and optimizing the cross section in terms of the thickness of the walls and the layout of the reinforcement. Fig. 1 shows the plan and a 3D sketch of the existing basin. Each wall is identified by a number since a structural analysis has been developed for each of them according to the specific loading conditions. The structure consists of perimeter walls and septa that divide it into individual tank cells. Wall 1 has a total height of 4.87 m, while Wall 3 and Wall 2 measure 3.00 m and Walls 4 vary in height from 3.00 mm to 4.87 m. The service scenario for this type of structures, which are built partially underground, includes the soil thrust, traffic overload and the pressure of the water, which is characterized, among the others, by an average content of chlorides equal to 10 g/L in line with [22].

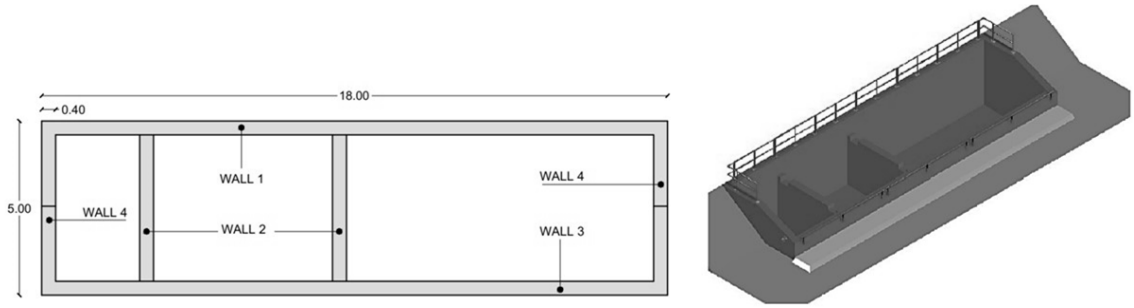

Figure 1: Layout (left) and 3D model (right) of the existing basin structure according to [26]

2.1 Loading conditions and structural analysis

Since the structure is built partially underground and has to contain water, its walls have to be designed to withstand, as above mentioned, the soil thrust from outside and the water hydraulic pressure from inside. Two different kind of soils, the characteristics of which are reported in Table 1, have been hypothesized in the design according to [26]: a filling soil, that is only in contact with Wall 1 of Fig.1 and a compacted foundation soil which is in contact with Walls 4 and Wall 3. This is due to the morphology of the site where the basin is supposed to be located, in a zone with different altitudes that requires to import reclaimed soil alongside Wall 1. The water table is always considered at 2 m depth for the sake of simplicity and in line with the geotechnical reports in [26].

Table 1: Characteristics of the soil

		Filling soil	**Foundation soil**
Specific weight	γ_{sat} [kN/m^3]	13	17
Internal friction angle	ϕ'_k [°]	20	33

The four walls have been designed to withstand the following combination of actions: i) Wall 1 and Walls 4: the soil thrust, the water hydraulic pressure and the self-weight; ii) Walls 2: the water hydraulic pressure and the self-weight; iii) Wall 3 is subjected to the same actions as Wall 1, plus the machinery traffic overload for which an excavator, with the weight equal to 94 tons, according to the producer's technical sheet [27], has been taken into consideration and has been assumed as the only variable action, all the other ones being permanent.

The structural analysis has been developed according to the following hypotheses: i) each wall is modelled as a cantilever beam considering a unit (1m) width; ii) soil pressure is estimated by means of the Rankine theory as per Eurocode 7 and through the parameters in Table 1; iii) each wall is subjected to the worst loading conditions for both Ultimate Limit State (ULS) and Serviceability Limit State (SLS) in favour of safety, which correspond, for Walls 1, Wall 3 and Wall 4, to the empty basin (soil thrust and machinery variable overload) and for Wall 2 to the presence of water only in one of the tank compartments.

Table 2 reports the design values of the bending moment (M_{Ed}) and axial force (N_{Ed}) which have been calculated as acting on each wall critical cross section according to the worst combination of actions. Fig. 2 reports the design models used for Wall 1, Walls 2, Wall 3 and Wall 4 that differ from each other by the presence of the action of the soil and of the water.

Table 2: Design actions for each wall (worst combination)

	M_{Ed} [kNm]	N_{Ed} [kN]
Wall 1	84.26	49.90
Wall 2	58.50	30.51
Wall 3	68.83	30.51
Walls 4	63.60	49.90

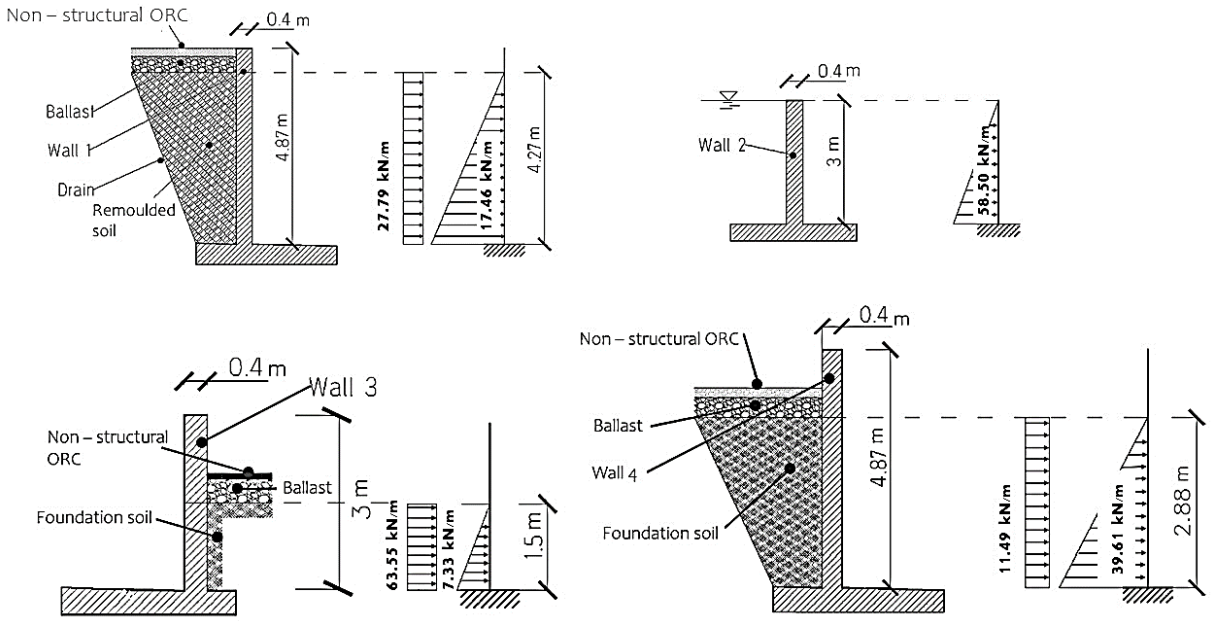

Figure 2: Representation of the structure and of the related structural design models for Wall 1 and Wall 2 (top part, left and right side respectively) and Wall 3 and Wall 4 (bottom part, left and right side respectively). While a triangular distribution has been assumed for the soil and for the water, a rectangular one has been employed for the other actions. An average loaded portion between Wall 1 and Wall 3 has been considered for Wall 4, due to the fact that its height passes from 4.87 m to 3 m.

2.2 Ordinary reinforced concrete basin design

Given the characteristics of the environment which surrounds the structure, the corresponding exposure classes have first been identified to define the prescriptions provided by the current standards [28]: XS2 (corrosion induced by chlorides from seawater for a permanently submerged element) and XA3 (highly aggressive chemical environment). The XA3 exposure class is due to the presence of $S_2O_3^{2-}$, SO_3^{2-}, SO_4^{2-} and H_2S expected to have a concentration equal to 46 mg/L, 325 mg/L, 5.1 mg/L and 1.5 mg/L respectively as in [22]. The XA3 class imposes a minimum C35/45 strength class, with a maximum water to binder ratio equal to 0.45 and a minimum cement content equal to 350 kg/m^3. To fulfill these prescriptions, the mix design reported in Table 3 has been employed for the ordinary reinforced concrete structure herein assessed. Furthermore, the analysis considered the following values: a characteristic compressive strength of 35 MPa, a mean concrete tensile strength of 3.20 MPa, and a Young modulus of 34 GPa.

Table 3: ORC mix design (in kg/m^3)

	ORC
Cement I 42.5 R	370
Water	150
Aggregate 7/10	354
Aggregate 12/20	377
Natural Sand (0-2 mm)	1108
Superplasticizer	3

Moreover, the Eurocode provides not only minimum material composition requirements but also structural prescriptions such as minimum concrete cover, to ensure the protection of the steel against the corrosion, and a minimum reinforcement

area, for exquisite structural performance purposes. While 40 mm had to be guaranteed as a minimum concrete cover due to the exposure classes above mentioned, the minimum vertical reinforcement area had to range between 0.002 Ac and 0.04 Ac, Ac being the cross sectional area of concrete. Similarly, the cross sectional area of the horizontal reinforcement had to be higher than 25% of the vertical reinforcement area and 0.001 Ac, whichever larger. This lead then to design a 400 mm thick cross section for the ordinary reinforced concrete basin as the one reported in Fig. 3. The design philosophy which governed the dimensioning has been structured to ensure a simple construction phase according to the following principles: i) reinforcement bars duplicated at both tension and compression side (longitudinal Φ 10 every 125 mm and transversal Φ 10 every 250 mm) due to the need of having a minimum ductility. For the sake of simplicity, the reinforcement at the compression zone has been then designed equal to the tensile one; ii) small diameters of the reinforcement bars to facilitate their handling.

With regard to the SLS, the stress limitation, crack control and deflection control have been taken into consideration. The design governing limit state is the crack width control (a maximum crack opening equal to w_k=0.2 mm has been enforced); deformation control, with a top edge deflection equal to 1/200 of the wall height, has been also enforced for the sake of integrity of the supported superstructure. Moreover, the mix design of Table 3 being characterized by an average tensile strength equal to 3.2 MPa, and the maximum tensile stress resulting from linear elastic calculations being equal to 5.2 MPa, cracked cross section assumptions have been made in the design calculations. The axial load to the wall self-weight was not able to keep the cross section within the decompression or at least within the crack formation SLS. This obviously was reflected in the related assumptions on the values of durability parameters, including e.g., chloride diffusion coefficient and the cracked state representing preferential paths for the ingress of harmful substances from outside. The ordinary reinforced concrete structure is herein after referred as Basin_ORC.

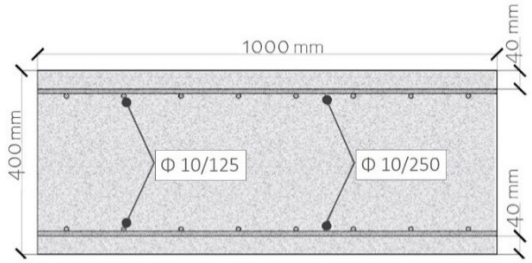

Figure 3: Cross section of the wall of Basin_ORC

2.3 UHPC basin – mix designs properties and proposed structural solutions

With reference to the UHPC basin, two different mix designs, UHPC1 and UHPC2 (to check whether a different material composition leads to different environmental consequences), are reported in Table 4 and two possible structural solutions are hereinafter proposed. The first one consists of cast in situ cantilever walls while, in the second case, the walls are made of, and designed as, precast UHPC panels supported by ordinary reinforced concrete buttresses. Both UHPC structural solutions have been designed following fib Model Code 2010 provisions on ULS and SLS as initial stage, also considering that UHPC automatically fulfills the EN 206-1 "deemed to satisfy" composition prescriptions with reference to durability [29][28]. As a matter of fact, water to cement ratio (equal to 0.33 for both mixes), strength class (compressive strength higher than 100 MPa, ranging from 126.9 MPa to 147.6 MPa depending on the specific mix design, as in [22][30]) and minimum cement content (600 kg/m³ or 700 kg/m³ for the cases here assessed) are already in line with the prescriptions for XS2 and XA3 exposure classes identified for the current case study [31]. Besides these aspects, UHPC, in comparison to conventional solutions, allows to reduce the minimum concrete cover (down to 25 mm as assumed for the case study at issue) due to its high tensile capacity, ductility and enhanced durability [32].

Table 4: UHPC1 and UHPC2 mix designs (in kg/m^3)

	UHPC1	**UHPC2**
Cement 52.5 R	700	600
Silica Fume	400	-
Slag	-	500
Water	231	200
Natural Sand (0-2 mm)	817	982
Superplasticizer (ACE 442)	64	33
Steel fibers (l_f=22 mm, d_f=0.2 mm)	160	120
Crystalline admixture	5.6	4.8

2.4 UHPC basin – structural design

The first designed structural scheme includes reinforcing steel bars only on the tension side to reach consistent advantages in terms of walls thickness in comparison to Basin_ORC. This also in view of the fact that, differently than for ordinary reinforced concrete, it is here possible to avoid reinforcement in the compression zone since the properties of the material can already cope with the ductility requirement. This resulted into longitudinal Φ 14 mm steel bars spaced at 165 mm for Wall 1 and Wall 3 and at 200 mm for Wall 2 and Walls 4. Moreover, transversal Φ 8 mm bars every 1000 mm have been placed to purely favour the stability of the longitudinal reinforcement. The thickness of the walls varied case by case, being equal to 160 mm for Wall 1, 120 mm for Walls 2 and 130 mm for Wall 3 and Walls 4. Fig. 4 reports a schematic representation of the cross section adopted for the cast in situ walls solution while Table 5 reports the safety factors for each wall according to this design.

For the solution with precast slabs, the latter were designed to have a width of 2 m with the supporting columns characterized by a 200 mm wide cross section, the depth of which reduces from 400 mm at the base to 200 mm at the top. Moreover, if on the one hand the supporting buttresses can be designed employing a cantilever beam structural model, on the other hand, the slabs have been designed with three fixed edges and one free edge and employing the yield line methodology. [14]. A similar model is also described by Timoshenko and Woinowsky [33] but, due to the different loading conditions and to the possibility to have torsional moments in correspondence of the corners the Wood-Armer (WA) method has been used. Although WA methodology has been conceived for ordinary reinforced concrete, the presence of the steel fibers in UHPC, allowed to assume a ductile behaviour. This is mainly due to the tensile constitutive law of the material and to its documented tensile strain hardening behaviour. Therefore, at the first stage, a thickness equal to 70 mm for Wall 1, 80 mm for Wall 3 and 50 mm for both Walls 2 and Walls 4 has been assumed. The highest WA bending moment in absolute terms, reported in Table 6, has then been considered, due to the uniformity of the slab. With regard to the buttresses, which are not only subjected to the external loads (e.g. soil, water) but also to the reaction forced transmitted to them by the supported slabs, a cantilever beam has been employed as a structural scheme. Table 7 reports the calculated bending moment acting on the buttresses where MEd,ext is the calculated acting bending moment on the panels and MEd,reaction refers to the reaction forces transferred from the latter in correspondence of the column (counted twice since two walls insist on one buttress). Fig. 4 illustrates the cross section of the structure made with slabs and buttresses.

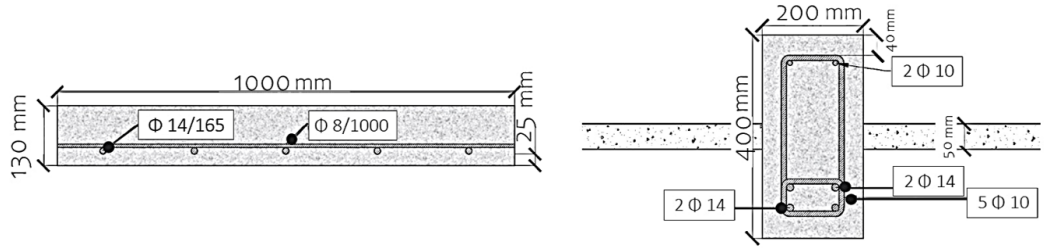

Figure 4: The picture illustrates two distinct design proposals for the basins, utilizing either UHPC1 or UHPC2. These options, both pertaining to Wall 4, are presented as follows: the uniform wall design (on the left) and the slabs supported by buttresses (on the right).

Table 5: Safety factors (M_{Rd}/M_{Ed}) for the initial proposed design

	M_{Rd}/M_{Ed}
Wall 1	1.04
Walls 2	1.03
Wall 3	1.09
Walls 4	1.05

Table 6: Wood-Armer bending moments in the panels

	$M_{WA,\,ab,\,max}$ [kNm]
Wall 1	6.35
Walls 2	5.95
Wall 3	13.66
Walls 4	4.76

Table 7: Design bending moments acting on the buttresses and applied to the cantilever beam structural model

	$M_{Ed,ext}$ [kNm]	$M_{Ed,reaction}$ [kNm]	$M_{Ed,tot}$ [kNm]
Wall 1	100.53	5.24	111.00
Walls 2	58.50	2.33	63.15
Wall 3	68.83	5.65	80.13
Walls 4	66.08	4.09	74.26

Both UHPC solutions have been verified at ULS and SLS. With regard to the ultimate limit state, the calculation of the resisting bending moment requires to explicit a constitutive law for both compression and tension. A stress block model (as for ordinary reinforced concrete) has been used in compression (considering a concrete class C100/120) while for tensile behaviour, reference was made to the research of Lo Monte and Ferrara [34] and following the guidelines of the fib Model Code 2010 [35], a simplified elastic perfectly plastic constitutive law was adopted, as identified from back analysis of the results of 4-point bending tests [36]. Table 8 summarizes the main UHPC design parameters then employed for the scope of this research and deduced from [34]. For the case of Basin_2_UHPC1 and Basin_2_UHPC2, the ULS calculations carried out for the UHPC panels also considered a transient design situation which included the lifting and handling of the precast slabs. With regard to the SLS, the compression stress limitation below 0.6 f_{ck} or 0.45 f_{ck} depending on the combination of actions), crack width limits ($w_{k,lim}$= 0.2 mm according to [36]) and deflection (l/200 as in [36], where l is the loaded height of the wall) have been checked in line with what has been reported in [37].

***Table 8**:* Main UHPC design parameters

$\mathbf{f_{ck}}$ characteristic compressive strength	100 [MPa]
$\mathbf{f_{ct}}$ tensile strength)	7.5 [MPa]
E (Young modulus)	41.7 [GPa]
ε_{peak} (ultimate tensile strain)	0.005

2.5 Corrosion

The corrosion and its effects on the overall durability of the assessed structures have been a key point of the study due to the environment rich in chlorides the tank walls are exposed to that can penetrate the concrete structure leading to the initiation and propagation of the corrosion. This is in line with the expectations since other researchers [13] already outlined how a Cl^- concentration might reach values as high as 213 mg/l, considered critical for geothermal power plants similar to the one here assessed. Moreover, it is worth observing that, for the case here analyzed, the depassivation and the consequent corrosion start from the part of the walls in contact with the water, since the soil is assumed to have a negligible chloride content. On the other hand, the carbonate ions coming from the permeated rainwater can potentially reach the surface of the wall, but, in line with [38], they are considered as unable of triggering a carbonation process since the structure is in contact with the soil and, then, the concrete can be hypothesized in saturated conditions. The ingress of chloride ions through the concrete matrix is governed by the process of diffusion that follows the second Fick' law. In this regard, a critical chloride concentration C_{crit}, of 0.44% by weight of cement (namely the concentration to be reached for the beginning of the propagation period) has been assumed, according to Alonso et al. [39]. The latter was based on field exposure tests which defined a depassivation chloride threshold that can vary from 0.3 % up to 3.5%. Another key role in the 2nd Fick's law is played by D_{app}, the apparent chloride diffusion coefficient, whose values, as already detailed in other works [8][40], might significantly affect the initiation time. A value of 10^{-11} m^2/s is generally used for the case of uncracked concrete containing CEM I [13][41][42][43] although, considering the microcracking initial state already described in 2.2 and caused by shrinkage, it has been set one order of magnitude higher and equal to 10^{-10} m^2/s for Basin_ORC. A value of 5 x 10^{-13} m^2/s has been taken into consideration for the structures made with UHPC_1 and UHPC_2 because of the compact matrix with much lower porosity but also in compliance with international standards, including, e.g., the French National Annex of EC2 [36] and the Swiss standard BFUP (Béton Fibrés Ultra Hautes Performance) [44][30][45]. Right after the initiation period, namely when at the level of the reinforcement (whose value can vary case by case as detailed in 2.5.1 and 2.5.2) the C_{crit} above mentioned is reached, the corrosion propagation stage starts and the steel bars start being corroded. As already done in similar studies, two different corrosion mechanisms have been assessed for the reinforcing bars within this research to have a more complete vision of what could happen in reality: a uniform one and a localized one. The uniform corrosion is considered to uniformly affect the surface of the steel bars with a speed which is mainly dependent on chloride content of the solution and relative humidity (RH). It has been assumed equal to 100 µm per year according to what has been reported by Bertolini in [9] and [10] for the case of concrete contaminated by chlorides with a RH higher than 90%. On the other hand, a hemispherical pit model was employed to describe a more aggressive phenomenon where mass and volume loss of steel are concentrated in a localized zone . This model assumes that the corrosion starts at a certain location of the reinforcement steel bar generating a pit

damage with an hemispherical shape [46][47]. Van Belleghem [46] carried out an experimental campaign aimed at representing a chloride environment with a typical NaCl concentration such as the marine one (33 g/L) exposing uncracked, cracked and cracked-&-healed concrete specimens to a series of wet and dry cycles. The author then developed a model to predict the loss of volume which can been calculated according to Eq. 2 integrating the pit area A_{pit} at a certain distance ξ from the center of the pit across an interval ranging from -p to +p (with p assumed as the depth of the pit). This allowed to compute a volume loss equal to 30.54 mm^3/year.

$$V_{pit} = \int_{-p}^{p} A_{pit}(\xi) \cdot d\xi \qquad \text{Eq. [2]}$$

Moreover, despite other studies [48] outlined how the damage to steel bars could be shaped in needle-like pits in early stage of chloride induced corrosion, it was anyway described that the damage occurs in a localized area with a length no longer than twice the diameter of the bars. In view of this, the use of a model aimed at describing a perfect hemispherical pit, like the one above mentioned, is considered as the one closest to the reality.

On the other hand, while the corrosion process of steel bars has been extensively studied and analysed, the corrosion of the steel fibres embedded into the concrete matrix is still debated, making the prediction of the degradation phenomena more difficult for UHPC. It is worth noting that Balouch et al. [49] concluded that, under alternated cycles of salt fog and drying, with a w/c ratio of 0.78, the fibres protected from the external environment by a maximum concrete cover thickness of 1 mm present corrosion spots on the surface. On the opposite, when the w/c drops to 0.5, a thickness of 0.02 mm is already sufficient to prevent such phenomenon. At the same time, the increased roughness, which is a corrosion effect, can improve the frictional interaction between the matrix and the fibres enhancing the tensile strength and toughness of the material. Other findings, as in [50] point out that the potential formation of healing particles in correspondence of the severely damaged fibre-concrete matrix interface, greatly improve the friction phase of the bond-slip behaviour, leading to a higher residual capacity in comparison to non-pre-slipped samples. Further works [51], assessing the corrosion attack through the crack of the fibres caused by a NaCl marine environment (with a concentration of 35 g/l), observed that the fibres (0.8 mm of diameter) within a rim 2 to 3 mm wide from the external surface of the samples were severely corroded. Out of this perimeter, the fibres presented a light corrosion without any reduction of their cross section. In line with this result, other experiments [52][53][54][55][56] pointed out the rapid corrosion for the fibres located within 10 mm from the exposed surface regardless of the exposure period and testing an environment characterized by a chloride concentration up to 35 g/L of NaCl with an exposure time ranging from 67 days up to 5 years. In view of this, as better explained in 2.5.2, the worst case scenario has been taken into consideration for the LCA and LCC purpose, assuming that fibres are immediately corroded as soon as the critical chloride concentration of above is reached (0.44% by weight of cement).

2.5.1 Steel reinforcement corrosion in ordinary reinforced concrete basins

As from the models summarized above, the time to corrode a given percentage of steel reinforcement bars has been then calculated, with the aim of estimating when to carry out appropriate maintenance works to restore the functionality of the ORC structures. Both the initiation time and propagation rate (uniform or hemispherical alternatively) have been computed according to what has been described in 2.5. As a matter of fact, due to the thickness of the walls of Basin_ORC, service conditions concerning deflections and stresses are negligible while crack opening is more impactful. Bossio et al. [57] addressed this problem linking the crack opening to corrosion propagation along and across a steel bar. Thus, it is assumed that once a loss of reinforcement area in the range 16-25% (on a single line of bars) is reached, the consequent expansion due to corrosion products is likely to result into a crack opening 0.5-1 mm wide. The latter is considered as able to disrupt the serviceability of the structure with the consequent need for major maintenance activities. Hence, for the scope of the analysis, in line with [8] and the estimations by [58], which stated that a loss higher than 15% causes a critical concrete damage able to affect the structural capacity of reinforced concrete, a value of 20% of loss of the reinforcement bar has been deemed as critical. Therefore, the time needed to reach this value has been estimated for each wall of Basin_ORC, together with the variation over time of the resistant bending moment M_{Rd} at the critical cross section of the cantilever , in order to further check the structural capacity variation. Assuming a value equal to 40 mm as x_{crit} in the 2nd Fick' law detailed in 2.5, namely the concrete cover of Basin_ORC walls, and keeping the values above listed for C_{crit}, and D_{app}, an initiation time of 0.3 years has been calculated to depassivate the reinforcement steel bars surface. Consequently, 6 and 3 years are the estimated times to lose 20% of the cross section of the bars employing the uniform corrosion assumption (100 µm/year) and the hemispherical pit model respectively (30.5 mm^3/year) including the initiation period. In these calculations a key role is played by the D_{app} value. As stated before, due to the microcracking state of ordinary reinforced concrete basins, 10^{-10} m^2/s has been accounted, while a value simply one order of magnitude lower (namely 10^{-11} m^2/s, as typical for uncracked ORC) would have led to a completely different initiation time, namely 2 years instead of 0.3 years. Basin_ORC subjected to the uniform corrosion is hereinafter referred as Basin_ORC_U while the one affected by the hemispherical pit corrosion is indicated as Basin_ORC_H. Fig. 5 reports an example of the evolution over time of Wall 1 resistant bending moments (M_{Rd}), according to both forms of corrosion. It can be observed that the threshold to compute the moment when the maintenance activities have to be carried out is related to a situation when the structural capacity is still ensured ($M_{Rd} > M_{Ed}$). Table 9 summarizes the time spans, calculated as above and needed for each of the walls of Basin_ORC_U and Basin_ORC_H to achieve a situation

where the resistant bending moment decreases down to the value of the design bending moment due to the relevant combination of actions, highlighting an occurrence of the event anyway not too delayed in the life time of the assessed structure.

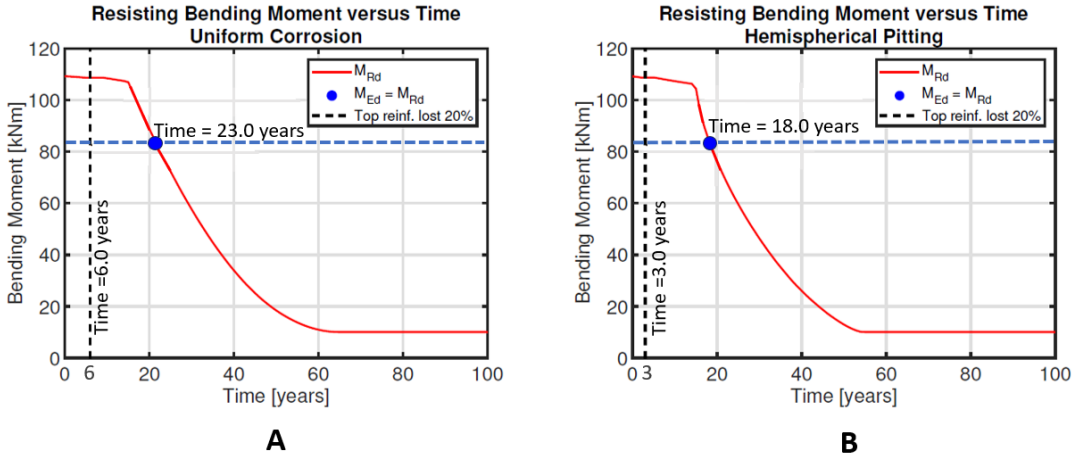

Figure 5: Wall 1 resisting bending moment within 100 years for Basin_ORC_U (A) and Basin_ORC_H (B)

Table 9: time needed to have M_{Ed} equivalent to M_{Rd} for Basin_ORC_U and Basin_ORC_H

	Basin_ORC_U	Basin_ORC_H
Wall 1	23 years	18 years
Wall 2	29 years	25 years
Wall 3	25 years	21 years
Wall 4	28 years	23 years

2.5.2 UHPC fibers and steel reinforcement corrosion

As stated in 2.5, the corrosion of the fibers which are uniformly distributed in the whole UHPC matrix is a topic that is still under investigation in the scientific literature. As a matter of fact, UHPC being a composite material, an overall integral degradation model must be employed to check its behaviour within the SL. For the scope of this research, the most severe condition has been taken into consideration, assuming immediate corrosion of the steel fibers once they are in contact with the chlorides and the critical chloride concentration (C_{crit}) is reached. This, because of their negligible size and not computing, then, a propagation period. According to this, the corrosion model assumed for the scope of this research defines a moving frontier of chlorides that have reached the critical threshold (the depth of which is estimated by means of 2nd Fick' law) and all the material within this frontier is disregarded in the calculations as usually done, e.g., for the design of timber structures in fire scenarios [59]. This is a quite severe assumption and, however, it should be noted that in the case of UHPC, as an advantage in comparison to other materials, the tendency to have narrower crack widths can potentially delay the corrosion process. Furthermore, it is worth remarking that recent studies [22,60,61] have demonstrated the delay in terms of chlorides penetration due to the autogenous self-healing properties, also favoured by the presence of crystalline admixture even for quite high values of initial crack openings (up to 0.5 mm). These same self-healing capacity is able to compensate for early age cracking, e.g. due to restrained shrinkage**.** Thus, different and more realistic approaches are possible like the one by Davolio et al. [62] and by Al Obaidi et al. [32] that assessed the flexural performance of UHPC slabs under simultaneous environmental and mechanical loading by implementing an experimentally calibrated constitutive law, evolving as a function of competing degradation and self-healing phenomena. The experiments were carried out by submerging thin beams (100 mm wide x 500 mm long x 30 mm thick) into geothermal water while keeping them under sustained loading through a dedicated testing rig; after having tested them up to failure at the end of prescribed exposure periods, the exposure-time affected constitutive law was obtained by using an inverse analysis procedure already employed in other studies [63]. Nonetheless, being aware that methods more conservative as the latter may need a proper modelling calibration to be extrapolated to the potentially much longer estimated service lives for UHPC [64], for the sake of ordinary reinforced concrete vs UHPC comparison the most aggressive condition (moving chloride frontier and layer removal) has been taken into consideration for the analysis reported in the following. In addition, since the structural solution with UHPC uniform walls has been supposed to also include reinforcing steel bars, the potential corrosion of the latter has been assessed employing the

same procedure as in 2.5.1 but using a D_{app} value of 10^{-13} m^2/s for UHPC. It was thus possible to estimate that these bars are never reached by the chlorides within the pre-determined service life period.

2.6 Durability Assessment-Based Design

In general, the approach encompassed by the design codes is based on the idea that the concrete is a passive provider of protection rather than an active player in the degradation phenomena, without considering, then, the evolution over time of its performance and the resulting outcomes on the time evolution of the structural performance as well. Moreover, most of the current codes have been developed with reference to conventional ordinary reinforced concrete, with mechanical and durability characteristics that are completely different from those of UHPC. Thus, in line with the definition of the durability as the capacity to fulfill the performance requirements without unforeseen expenditure on maintenance and repair over the intended service life, as proposed by the fib Model Code 2010 [37], the evolution along time of the material performance has been assessed according to what has been stated in 2.5.2 to calculate the serviceability and the ultimate structural performance. As a first step, following the structural consideration proposed in 2.3, the UHPC structures have been designed with the dimensions of the wall and of the slabs reported in the following Table 10. Moreover, no differentiation has been made in terms of the type of corrosion for the basins with uniform walls, as it is estimated that the reinforcement steel bars are not exposed to chlorides. These walls are henceforth referred to as Basin_1_UHPC1 and Basin_1_UHPC2, depending on whether they are constructed with UHPC1 or UHPC2, respectively. However, this approach was not replicable for the structure consisting of precast UHPC slabs and ORC columns. Consequently, the latter are assumed to follow the same considerations as the ordinary reinforced concrete elements described in section 2.5.1. This has to designate the structure subject to uniform corrosion of the columns as Basin_2_UHPC1_U and Basin_2_UHPC2_U, depending on whether they are constructed with UHPC1 or UHPC2, respectively. Similarly, the terminology Basin_2_UHPC1_H or Basin_2_UHPC2_H will be hereinafter used when the reinforcement is modeled as being subject to the same hemispherical pit corrosion mechanism as the ORC elements, and the UHPC elements are cast with UHPC1 or UHPC2 respectively.

Table 10: Time needed to have $M_{Ed}=M_{Rd}$ for each wall of Basin_1_UHPC1, Basin_1_UHPC2, Basin_2_UHPC1_U, Basin_2_UHPC2_U, Basin_2_UHPC1_H and Basin_2_UHPC2_H without DAD assumptions on a maximum number of maintenance activities

	Basin_1_UHPC1 and Basin_1_UHPC2		**Basin_2_UHPC1_U, Basin_2_UHPC2_U, Basin_2_UHPC1_H and Basin_2_UHPC2_H**	
	Thickness	**Time needed to have $M_{Ed}=M_{Rd}$**	**Thickness**	**Time needed to have $M_{Ed}=M_{Rd}$**
Wall 1	160 mm thick	1 year	70 mm thick	10 years
Walls 2	120 mm thick	1 year	50 mm thick	1 year
Wall 3	130 mm thick	2 years	80 mm thick	1 year
Wall 4	130 mm thick	1 year	50 mm thick	1 year

2.6.1 Durability Assessment-Based Design – rationale

It can be clearly observed, from the results summarized in Table 10, that the structural design performed as in section 2.5.2 without any consideration for the material degradation phenomena does not guarantee, at this stage and also considering the assumed reduction in reinforcement cover, adequate performance over the time. As a matter of fact, the calculated decrease of the resistant bending moment, because of corrosion degradation phenomena, resulted into an ultimate limit state achieved as early as after only one year (this being the time when the decreased M_{Rd} becomes equal to M_{Ed}). Fig. 6 gives an example in this regard with reference to Basin_1_UHPC1_1 and Basin_1_UHPC2. The latter registered a M_{Rd} value, at time 0, of 104.9 kNm, 60.5 kNm, 75.1kNm and 69.8 kNm for Wall 1, Wall 2, Wall 3 and Wall 4 respectively. These values are respectively decreased up to 100.5 kNm, 58.5 kNm, 68.8 kNm and 66.1 kNm after mostly 1 year. Similarly, Basin_2_UHPC1_U, Basin_2_UHPC2_U, Basin_2_UHPC1_H and, Basin_2_UHPC2_H start from the values of M_{Rd} equal to 104.9 kNm, 60.5 kNm, 75.15 kNm and 68.8 kNm for Wall 1, Wall 2, Wall 3 and Wall 4 respectively that are then lowered up to 58.5 kNm, 58.5 kNm, 68.8 kNm and 66.1 kNm because of the corrosion process.

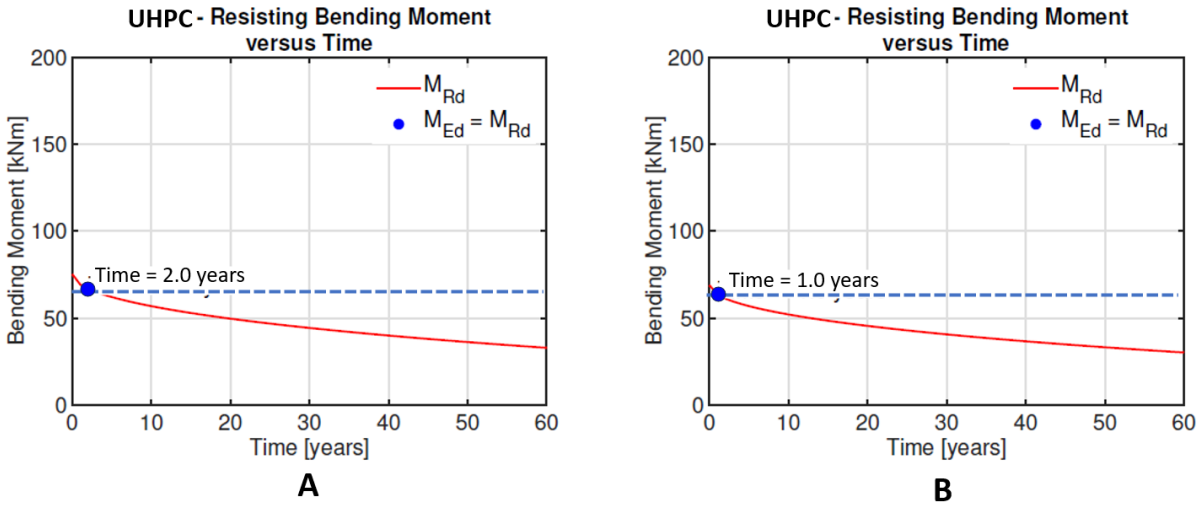

Figure 6: Resisting bending moment versus time for Wall 3 (A) and Wall 4 (B) of Basin_1_UHPC1 and Basin_1_UHPC_2

In view of this a DAD workflow (summarized in Figure 7) has been implemented to redesign the UHPC structure with the aim of achieving a performance such that the attainment of the ULS was delayed beyond the service life and with maximum one maintenance activity to be carried out within the 50 years of Service Life, due to the attainment of the relevant serviceability limit state.

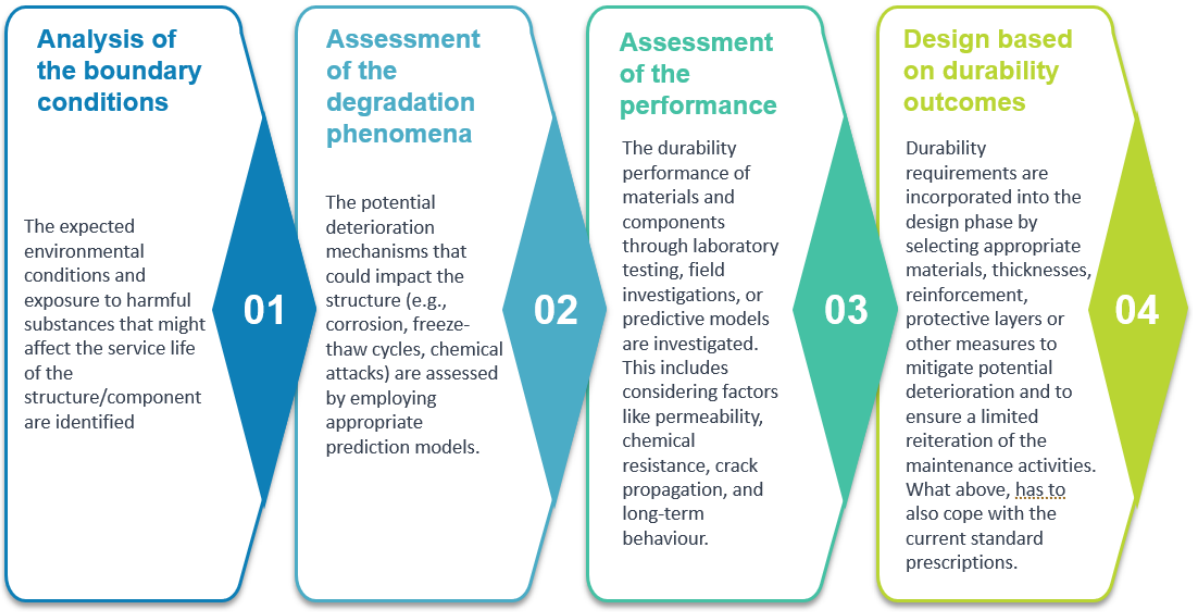

Figure 7 : Durability Assessment based Design workflow

For the latter, differently than ordinary reinforced concrete structures where the crack opening limit state was evaluated, maintenance activities have been scheduled for UHPC when a deflection of l/200 is exceeded, the structure being more slender. This, also in view of the fact that, working in the strain hardening regime for UHPC and due to the characteristics of the material, crack opening always less than 0.2 mm is expected. With regard to Basin_1_UHPC1 and Basin_2_UHPC2, designing a thickness of 190 mm for Wall 1, 150 mm for Wall 2 and Wall 3 and 160 mm for Wall 4, with longitudinal reinforcement bars of 14 mm, it was then possible to reach the goal above mentioned. As a matter of fact, the repairing activities are mainly dictated by Wall 4 since it reaches the deflection limit state at around 25 years of SL. In view of this, and even though it is estimated that the serviceability limit state is reached after 37, 31 and 92 years for Wall 1, Walls 2 and Wall 3 respectively, all of them are supposed to be maintained anyway at the age of 25 years for the sake of simplicity.

With reference to Basin_2_UHPC1_U, Basin_2_UHPC2_U, Basin_2_UHPC1_H and Basin_2_UHPC2_H, increasing the thickness of the walls up to 100 mm it is possible to avoid any kind of maintenance activity for the UHPC elements in line with

the aforesaid goal of the DAD approach. Table 11 indicates the improvements then obtained. Comparing Table 10 to Table 11 it is possible to highlight how a design purely based on durability prescription is not enough even for UHPC, as clarified by Table 10, since M_{Rd} reaches the M_{Ed} values after a short period. These outcomes also highlight how a design with a safety factor near to one (as demonstrated in Table 4), which is aimed at optimizing material usage, could anyway and potentially encounter certain durability concerns. Thus, an increase of the thickness up to the values of Table 11, besides ensuring a limited (for UHPC structures with uniform walls) or no (for other UHPC structures) amount of maintenance activities, also ensures a M_{Rd} always higher than M_{Ed}. Fig 8 shows, for the case of Wall 1, the bending moment versus time together with the tip deflection for Basin_UHPC1 as well as the resisting bending moment versus time for Basin_UHPC2_U and Basin_UHPC2_H.

Table 11: Time needed to have $M_{Ed}=M_{Rd}$ for each wall of Basin_1_UHPC1, Basin_1_UHPC2, Basin_2_UHPC1_U, Basin_2_UHPC2_U, Basin_2_UHPC1_H and Basin_2_UHPC2_H with DAD assumptions on a maximum number of maintenance activities

	Basin_1_UHPC1 and Basin_1_UHPC2			Basin_2_UHPC1_U, Basin_2_UHPC2_U, Basin_2_UHPC1_H and Basin_2_UHPC2_H		
	Thickness	Time needed to have $M_{Ed}=M_{Rd}$	Number of additional years in comparison the previous design	Thickness	Time needed to have $M_{Ed}=M_{Rd}$	Number of additional years in comparison the previous design
Wall 1	190 mm thick	58 years	+ 57 years	100 mm thick	62 years	+ 52 years
Walls 2	160 mm thick	56 years	+ 55 years	100 mm thick	68 years	+ 67 years
Wall 3	160 mm thick	53 years	+ 51 years	100 mm thick	50 years	+ 49 years
Wall 4	160 mm thick	61 years	+ 60 years	100 mm thick	82 years	+ 81 years

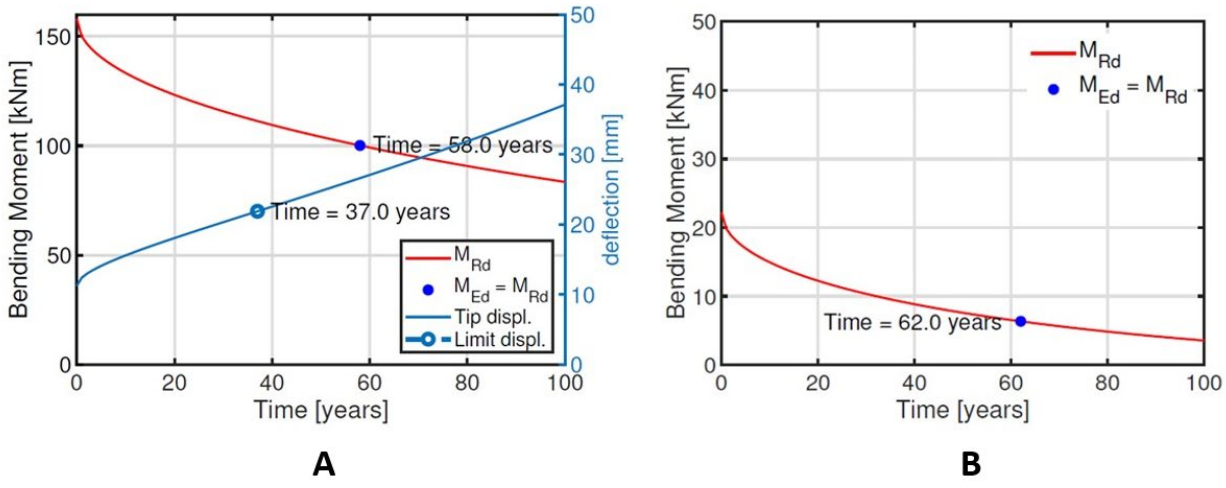

Figure 8: Bending moment and top deflection vs time for Wall 1 of Basin_1_UHPC1 and Basin_1_UHPC2 (A). Bending moment vs time for Basin_2_UHPC1_U, Basin_2_UHPC2_U, Basin_2_UHPC1_H and Basin_2_UHPC2_H (B).

3 The Influence of DAD on LCA and LCC outcomes

3.1 LCA and LCC - system boundaries

The assumptions made in the previous sections represent the input for the sustainability analyses hereinafter described. More specifically, the latter have been carried out according to ISO 14040-14044 following the four main steps: i) definition of the goal and scope, ii) inventory analysis, iii) impact analysis and iv) interpretation [65][66]. Thus, since the main aim of the research is to identify the most convenient solution in terms of costs and environmental implications, the assessed Functional Units (FU) have been always the whole basins reported in Table 9, built employing the different materials and according to the different structural concepts as above, whereas the different degradation models, namely uniform and

pitting corrosion, do enter into the assessment of the maintenance activities. A 50 year service life (SL) has been hypothesized, complying with code prescriptions [28]. Moreover, a cradle-to-grave system boundary has been fixed including the use stage of the structures as well as the reiteration of the retrofitting activities whenever needed. Then, all the impacts and the costs starting from A1 phase (extraction of raw materials) up to D (reuse/recovery/recycling potential) of EN15805 standard [67] have been accounted. The maintenance activities assessed for Basin_ORC_U and Basin_ORC_H consist of the removal of the concrete cover and of the corroded steel bars with the consequent substitution of the latter and the subsequent reconstruction of the cover layer by means of forms and cast-in-place concrete. The waterproofing of the ordinary reinforced concrete basin, as usually done in the current practice, has been considered as made of a bituminous emulsion applied by brushing in the amount of 1,500 g/m^2 without any pre-treatment of the concrete surface. The impacts associated with this layer have been estimated by means of the Environmental Product Declaration (EPD) developed for similar commercial products [68]. In this respect, it must be remarked that various repairing strategies are possible. However, the methodology usually employed for this type of structures is taken into consideration here, as confirmed by current practice for similar structures such as the one that this study aims to replicate in Italy. As stated above, the UHPC elements of Basin_1_UHPC1, Basin_1_UHPC2, Basin_2_UHPC1_U, Basin_2_UHPC2_U, Basin_2_UHPC1_H and Basin_2_UHPC2_H have been supposed not to require any steel replacement, also considering that in the case of Basin_1_UHPC1 and Basin_1_UHPC2, the reinforcement bars did not corrode within 50 years as detailed in 2.5. Therefore, as soon as the limit deflection is attained, the concrete contaminated by chlorides is replaced with the same procedure described for the ordinary reinforced concrete elements. No waterproof layers are needed for UHPC elements since the waterproofing performance is ensured by the extremely reduced porosity of the UHPC, also thanks to the incorporation in its mix-design of the crystalline admixture, which served as porosity reducers, as well as self-healing stimulator, this already assessed aspect being anyway beyond the scope of this paper[69]. Moreover, while the concrete is always supposed to be treated as a waste material, steel scraps (deriving from fibers and reinforcing bars) are supposedly recycled in compliance with the current EU protocols on construction and demolition waste[70]. The LCA analysis has been developed using the CML-IA impact method released by the Center of Environmental Science (CML) of Leiden University in 2013. The ten assessed indicators are the ones reported in Fig. 9, namely global warming (GWP); acidification (AP); ozone depletion (ODP); photochemical oxidation (POCP); eutrophication (EP); abiotic depletion potential (ADP); human toxicity potential (HTP); freshwater aquatic ecotoxicity potential (FAETP); marine aquatic ecotoxicity (MAETP) and terrestrial ecotoxicity potential (TETP). SimaPro software, which employs the existing library Ecoinvent 3.6 as data source for most of the environmental burdens associated with raw components, has been used for the scope of the environmental calculations. LCC has been performed employing the prices reported in the Italian construction costs list [71] [72] or, alternatively, carrying out a market survey to collect the missing ones. Costs of the activities to be developed in the future have been estimated by means of an interest rate calculated as in [8] and [73]. Table 12 give a brief overview of the concrete quantities accounted for the scope of this research while Table 13 lists the main construction rates employed for the cost estimation.

Table 12: total m^3 of concrete accounted for the scope of this research

	Basin_ORC_U	**Basin_ORC_H**	**Basin_1_UHPC1 and Basin_1_UHPC2**	**Basin_2_UHPC1_U and Basin_2_UHPC2_U**	**Basin_2_UHPC1_U and Basin_2_UHPC2_U**
m^3 of ORC	207.40 (including maintenance activities)	304.39 (including maintenance activities)	31.27 (including maintenance activities)	19.76	19.76
m^3 of UHDC	-	-	-	38.52 (due to the buttresses and their maintenance activities)	72.31 (due to the buttresses and their maintenance activities)

Table 13: main construction rates employed fort his investigation

Work	**Rate per unit (€)**	**unit**
Excavation works	5.79	m^3
Excavation works (depth 1.5 m – 3 m)	6.86	m^3
Excavation works (depth higher than 3 m)	12.33	m^3
Formworks	23.94	m^2
Formwork fees for heights from 4.51 m to 18 m	1.54	m^2
Casting of concrete C 12/15	103.01	m^3

Casting of concrete C 35/45	158.66	m^3
Casting of UHPC	430.00	m^3
Supply and installation of rebars	2.23	kg
Demolition of concrete	423.96	m^2
Backfilling and soil compacting	29.99	m^3

3.2 Results and discussion

The boundaries above described led to highlight the potential advantages, both in terms of environmental burdens and overall costs, of UHPC in comparison to ordinary reinforced concrete when used to build structures exposed to an aggressive environment. To better analyze the outcomes, each impact indicator has been broken down into 5 items: cement, steel, others and disposal/recycling. Noteworthy that steel includes both reinforcing bars and steel fibers while the item disposal/recycling includes at the same time the treatment of concrete debris as waste materials as well as the recycling of the steel scraps. As detailed in Fig. 9, most of the environmental impact indicators registered a reduction higher than 60% in the case of Basin_1_UHPC1 and Basin_1_UHPC2 when compared to the reference Basin_ORC_H. The only indicator that was observed having a limited advantage is the Photochemical Oxidation with values of reduction not higher than 34%. On the opposite, the Fresh Water Aquatic Ecotoxicity was estimated having the highest reduction with a value of 74% in comparison to the reference for Basin_1_UHPC1. Similarly, the lowest reduction can be observed for the Photochemical Oxidation as well when Basin_2_UHPC1_H and Basin 2_UHPC2_H are compared to Basin_ORC_H or when Basin_2_UHPC1_U and Basin_2_UHPC2_U are compared to Basin_ORC_U. Moreover, for the case of the latter UHPC structures, the highest reduction has been observed for Basin_2_UHPC2_U with impact reductions as high as 76% for Human Toxicity and Fresh Water Aquatic Ecotoxicity.

An exception to all of the values above reported is represented by the Abiotic Deplation for Basin_1_UHPC2, Basin_2_UHPC2_H and Basin_2_UHPC2_U which has been noted performing even worse when compared to the corresponding reference. This is due to the presence in the UHPC mix design of the blast furnace slag that, coming from the iron production process accounts for around 83% of the overall impact value. In this respect it must be highlighted that this result strongly depends on the allocation methodology employed within the Ecoinvent data library used to account the impacts of the material. Since such allocation could redistribute the environmental burdens based on the physical weight or on the economic worth, future refinements of the iron process as well as a variation of the economic value within the market could lead to a complete different situation in the future. On the contrary, all the basins made with UHPC1 registered important improvements for the same impact indicator, that is a result in contrast with similar researches [24]. This is due to an update of the Life Cycle Inventory (LCI) that allowed to pass from the data of the activated silica to ones of silica fume, the latter having been here employed as the most proper inventory for the specific mix design of UHPC1. In addition to this, it is worth to note that negative values in Fig. 9 are due to the recycling process of steel scraps.

In general, the influence of the cement on the overall impact is in between 10% and 25% except for Photochemical Oxidation, Eutrophication and Global warming where it is possible to observe values up to 63% as in Basin_ORC_U. There are no relevant differences between the influence of cement of ordinary reinforced concrete and UHPC structures. This also in view of the optimized design here employed. As matter of fact, just considering the cement content (370 kg/m^3 and 700 kg/m^3 for ORC and for UHPC2 respectively) and ignoring the influence of the repairing activities and of other elements (e.g. the buttresses), the reduced thickness of the walls, from 0.40 m to 0.1 m, favours a reduction of the total quantity per each square meter of the structure. It is indeed possible to calculate that one square meter of the wall contains 140 kg and 70 kg for the basin made with ORC and UHPC2 respectively. On the other hand, for the steel a discrepancy between ordinary reinforced concrete and UHPC basins is registered, with percentage of influence always lower for the latter. As an example, steel is cause of 97% of marine Aquatic Ecotoxicity for Basin_ORC_U while its influence for UHPC structures is in the range 50 % - 70%. This is a direct consequence of two factors, namely the reduced maintenance activities for UHPC basins and the recycling of the steel scraps. As a matter of fact, the environmental benefits of the recycling treatment, which involves large quantities of steel for ordinary reinforced concrete basins, are accounted with negative numerical values. This reduces the total numerical value of the indicators, increasing then the incidence referred to the steel provision.

The cost assessment, as in Fig. 10, highlights the same aforesaid advantages with consistent reductions higher than 42% and 46% when Basin_1_UHPC1 or Basin_1_UHPC2 and Basin_2_UHPC2_H are compared to Basin_ORC_H. It is therefore possible to observe that the most convenient solution is the one with UHPC precast slabs due to the lack of maintenance activities within the SL. Despite the different assessed cost per cubic meter of ordinary concrete and UHPC (around 160 and 430 euros respectively for the scope of this research), it is here possible to observe that cement and steel count for approximately the same percentage. This aligns with the observation that, unlike ordinary reinforced concrete where the reinforcement costs are not considered on a cubic meter scale, UHPC already includes the cost of the fibers. To better analyze the data, the overall

costs have been split into both the construction and the maintenance phases. Moreover, they have been broken down into concrete and steel (reinforcing bars and fibres) contributions besides the one referred to the activities to be carried out to ensure a perfect execution of the works, excluding the casting of concrete and the steel provision/assembling, grouped into the item others. As possible to observe in Fig. 10, for the ordinary reinforced concrete basins, while concrete generates 17% and 13% of the costs in the construction and the maintenance stages respectively, and the steel 16% and 9% within the same phases, UHPC registers similar values. More specifically, 16% and 19% in the construction, for the concrete, and 15% and 19% during the maintenance for the steel. In general, UHPC is found to be always the most economically convenient solution independently on the type of design and corrosion here assessed. These outcomes are in line with the most recent literature for self-healing advanced cementitious materials [74][24] but also with other researches that, assessing the economic impacts of water basin structures similar to the one here proposed, pointed out a cost advantage of UHPC of around 22% with comparison to the reference made up of ordinary reinforced concrete [75]. This was noticed, even when employing different boundary conditions such as a different waterproofing solutions (bituminous coating layer) or a recycling process of the concrete debris at the end of life stage.

The results herein obtained definitely highlight that the higher cement content and the higher price per unit volume of UHPC can be overcome by employing a tailored Durability Assessment-Based Design approach which at the same time allows to optimize the structural dimensions, and hence the consumption of materials, and the assess the evolution of the material and structural performance over the time, which results into a thorough and holistic evaluation of the improved sustainability performance. Fig. 11 summarizes these aspects making a comparison between the present work and the most recent ones [24][76][8], with the same boundary conditions (namely, extended cradle-to-gate system boundary) and focused on advanced cementitious materials with a self-healing potential also checking the potential sustainability improvements by replacing virgin aggregates with recycled ones[24]. It is furthermore worth highlighting that remarkable improvements have been observed also in similar case studies, for most of the environmental impact indicators, except for[24] whose results are affected by the recycling process numerically accounted with a negative value.

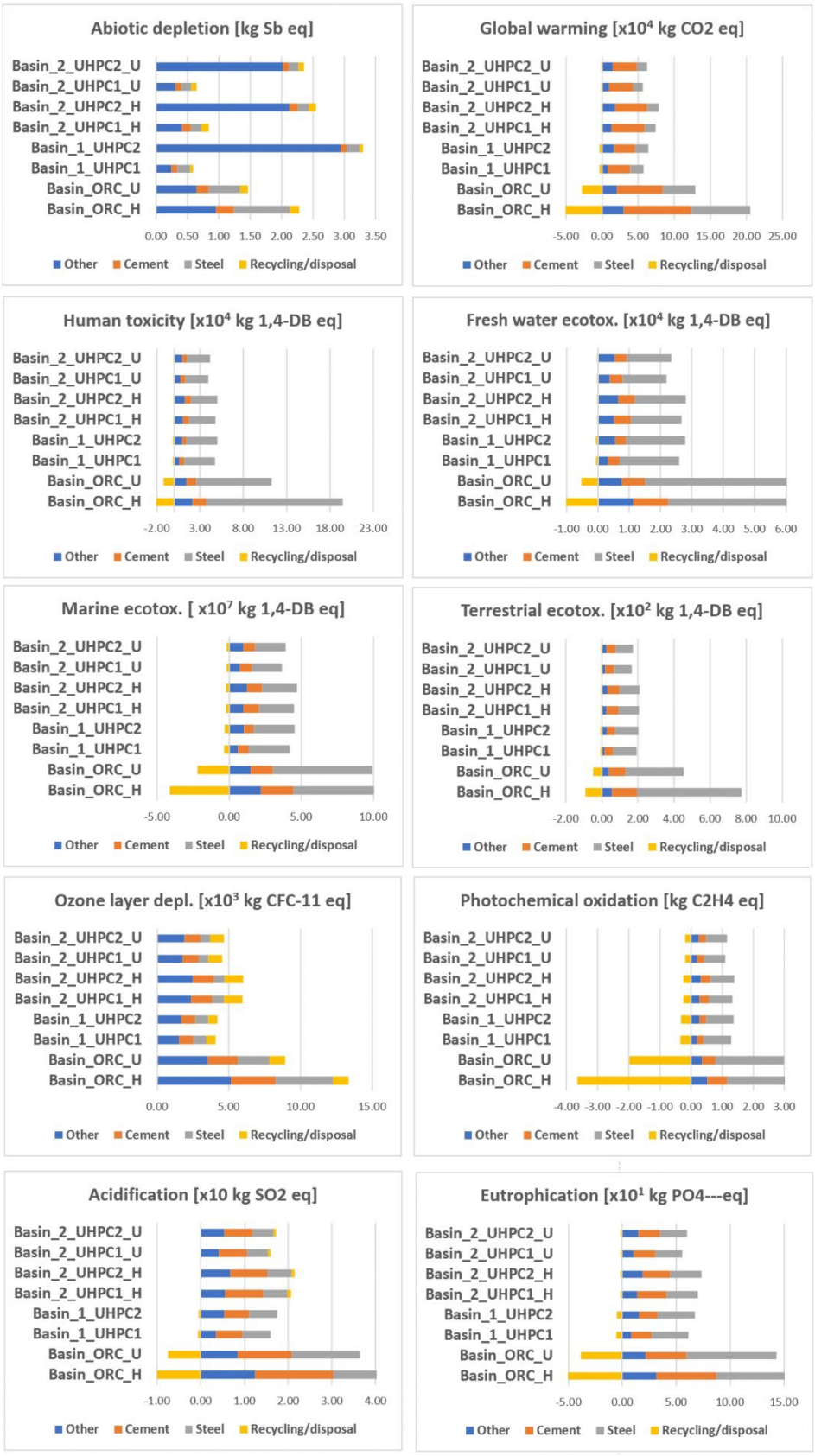

Figure 9: Comparison of environmental burdens for the ten CML-IA impact indicators. "Steel" is intended as inclusive of the reinforcement bars for ORC basins and of the steel fibers for the UHPC ones. "Other" includes all the components of the mix design, except for the cement, including the relative transport burdens and the energy consumed during the construction and the maintenance phase.

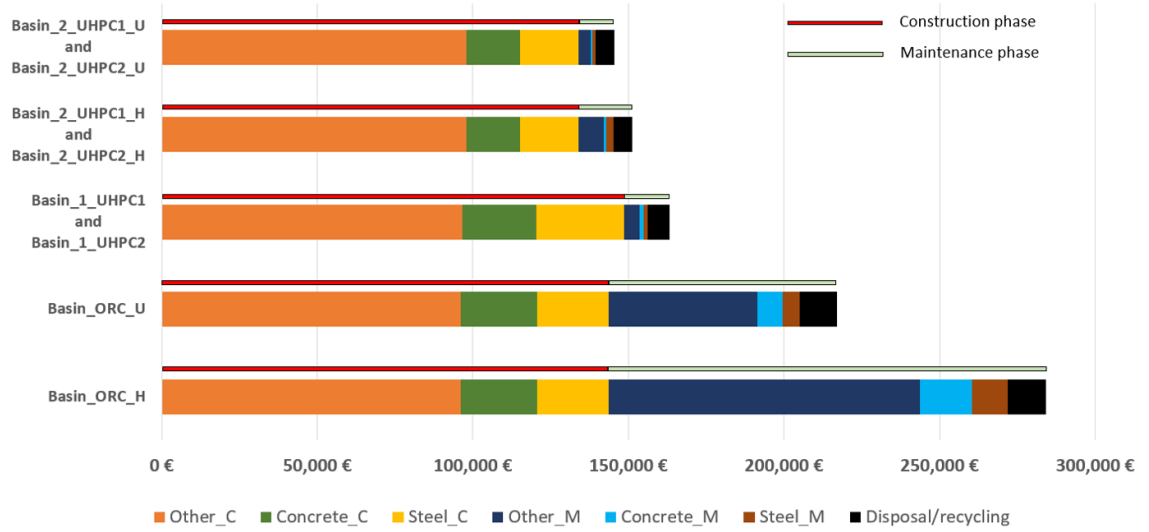

Figure 10: Comparison of overall costs within 50 years of SL. Other_C, Concrete_C and Steel_C are referring to the construction phase while Others_M, Concrete_M and Steel_M are related to the maintenance phases. "Steel" does include fibers for UHPC. "Others" includes all the activities to be carried out to ensure a perfect execution of the works, excluding the casting of concrete and the steel provision and assembling.

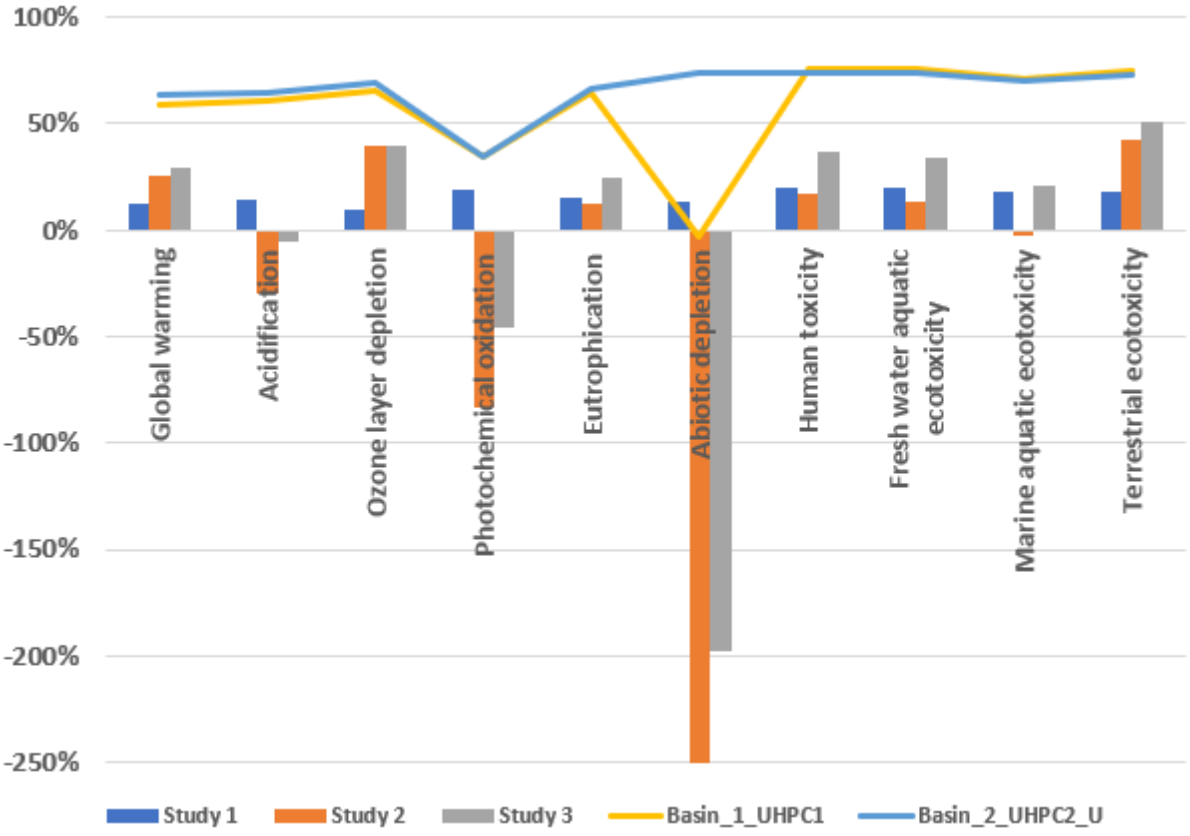

Figure 11: Reductions of environmental impacts for Basin_UHPC2_H in comparison to Basin_ORC_H. The reduction values, expressed in percentage, are obtained for concrete containing SuperAbsorbent Polymers (study 1, [8]), recycled-UHPC ([24]) and UHPC (study 3,[76]) in comparison to a reference solution. All of them are developed within an extended cradle-to-gate system boundary excluding the end-of-life stage.

4 Conclusions

The study has examined the incorporation of durability parameters into structural design workflows through the utilization of Durability Assessment-based Design (DAD) methodology, focusing on structures made with UHPC compared to ones made with ordinary reinforced concrete. The following main findings can be summarized:

- the current durability design approach for Ordinary Reinforced Concrete Structures, which primarily relies on "deemed to satisfy prescriptions" on minimum cement content, concrete cover, strength class, and maximum water/cement ratios can cause potential issues. As an example, the initial microcracking in ordinary reinforced concrete can lead to an increased chloride diffusion coefficient, fostering an early chloride penetration and a likewise early onset of the reinforcement corrosion, thereby resulting into earlier and more frequent maintenance;
- the DAD methodology proposed here allows for tailored scheduling of maintenance activities, optimizing structural design accordingly. It also offers advantages in terms of cost and environmental impact, especially for innovative cementitious materials like UHPC, which inherently perform better and whose benefits, since the deemed to satisfy prescriptions of current design codes are automatically satisfied, would and could hardly been appreciated otherwise;
- UHPC, while having higher costs and cement content per cubic meter compared to ordinary reinforced concrete, demonstrates better overall environmental and cost performance when considering structural applications, due to both the reduced volume of materials required to build the structure, for the same target performance, and the reduced maintenance frequency, respectively allowed and promoted by enhanced mechanical and durability performance;
- the assumption that fibers corrode immediately upon contact with chlorides represents a worst-case scenario for UHPC. A more in-depth examination of fiber corrosion could further improve UHPC outcomes;
- slabs built with UHPC containing slag show significant environmental reductions in Human Toxicity and Freshwater Aquatic Ecotoxicity but poorer performance in Abiotic Depletion when compared to the reference;
- uniform walls made with UHPC containing silica fume registered lower but similar reduction values to the previous case for both the economic and environmental performance when compared to the reference, but with consistent improvements for the Abiotic Depletion, mainly due to the substitution of slag with silica fume;
- the importance of employing quantitative tools like Life Cycle Assessment (LCA) to evaluate the influence of supplementary cementitious materials on overall sustainability and aid decision-making becomes clear.

Overall, these outcomes highlight how design approaches like the DAD herein proposed, can harness environmental, cost, and structural benefits from the outset, contributing to a more sustainable built environment and addressing social inequalities. This also implies the need to integrate the existing developments with a Social Life Cycle Assessment (SLCA) to establish a truly omni-comprehensive design approach that encompasses all relevant implications across various scales.

5 Acknowledgments

This project has received funding from the European Union's Horizon 2020 research and innovation programme under the Marie Skłodowska-Curie grant agreement No 860006

6 References

[1] Human Rights Council United Nations, Report of the Special Rapporteur on the issue of human rights obligations relating to the enjoyment of a safe, clean, healthy and sustainable environment, 2022.

[2] X. Zhao, J. Zuo, G. Wu, C. Huang, A bibliometric review of green building research 2000-2016, Archit Sci Rev. 62 (2019) 74–88. https://doi.org/10.1080/00038628.2018.1485548.

[3] European Commission, The European Construction Sector, Eur. Union, 2016, p. 16. http://ec.europa.eu/growth/sectors/construction/., (n.d.).

[4] L. Pérez-Lombard, J. Ortiz, C. Pout, A review on buildings energy consumption information, Energy Build. 40 (2008) 394–398. https://doi.org/10.1016/J.ENBUILD.2007.03.007.

[5] M. Yeheyis, K. Hewage, M.S. Alam, C. Eskicioglu, R. Sadiq, An overview of construction and demolition waste management in Canada: a lifecycle analysis approach to sustainability, Clean Technol Environ Policy. 15 (2013) 81–91. https://doi.org/10.1007/s10098-012-0481-6.

[6] S.A. Miller, V.M. John, S.A. Pacca, A. Horvath, Carbon dioxide reduction potential in the global cement industry by 2050, Cem Concr Res. 114 (2018) 115–124. https://doi.org/10.1016/J.CEMCONRES.2017.08.026.

[7] D.Y. Oh, T. Noguchi, R. Kitagaki, W.J. Park, CO2 emission reduction by reuse of building material waste in the Japanese cement industry, Renewable and Sustainable Energy Reviews. 38 (2014) 796–810. https://doi.org/10.1016/J.RSER.2014.07.036.

[8] D. di Summa, J.R. Tenório Filho, D. Snoeck, P. Van den Heede, S. Van Vlierberghe, L. Ferrara, N. De Belie, Environmental and economic sustainability of crack mitigation in reinforced concrete with SuperAbsorbent polymers (SAPs), J Clean Prod. 358 (2022). https://doi.org/10.1016/j.jclepro.2022.131998.

[9] L. Bartolini, M. Carsana, Materiali da costruzione, Citta` Studi, 2014.

[10] R.P.P. Luca Bertolini, Bernhard Elsener, Pietro Pedeferri, Corrosion of steel in concrete, 2004.

[11] D.M. Frangopol, K.-Y. Lin, A.C. Estes, Life-Cycle Cost Design of Deteriorating Structures, Journal of Structural Engineering. 123 (1997) 1390–1401. https://doi.org/10.1061/(ASCE)0733-9445(1997)123:10(1390).

[12] J. Liu, N. Farzadnia, K.H. Khayat, C. Shi, Effects of SAP characteristics on internal curing of UHPC matrix, Constr Build Mater. 280 (2021). https://doi.org/10.1016/j.conbuildmat.2021.122530.

[13] S. Al-Obaidi, P. Bamonte, L. Ferrara, M. Luchini, I. Mazzantini, Durability-based design of structures made with ultra-high-performance/ultra-high-durability concrete in extremely aggressive scenarios: Application to a geothermal water basin case study, Infrastructures (Basel). 5 (2020) 1–44. https://doi.org/10.3390/infrastructures5110102.

[14] S. Al Obaidi, P. Bamonte, F. Animato, F. Lo Monte, I. Mazzantini, M. Luchini, S. Scalari, L. Ferrara, Innovative design concept of cooling water tanks/basins in geothermal power plants using ultra-high-performance fiber-reinforced concrete with enhanced durability, Sustainability (Switzerland). 13 (2021). https://doi.org/10.3390/su13179826.

[15] N. De Belie, E. Gruyaert, A. Al-Tabbaa, P. Antonaci, C. Baera, D. Bajare, A. Darquennes, R. Davies, L. Ferrara, T. Jefferson, C. Litina, B. Miljevic, A. Otlewska, J. Ranogajec, M. Roig-Flores, K. Paine, P. Lukowski, P. Serna, J.-M.M. Tulliani, S. Vucetic, J. Wang, H.M. Jonkers, A Review of Self-Healing Concrete for Damage Management of Structures, Adv Mater Interfaces. 5 (2018) 1–28. https://doi.org/10.1002/admi.201800074.

[16] R. Folić, D. Zenunović, Durability problem of RC structures in Tuzla industrial zone - Two case studies, Eng Struct. 32 (2010) 1846–1860. https://doi.org/10.1016/j.engstruct.2010.03.004.

[17] J. Li, Z. Wu, C. Shi, Q. Yuan, Z. Zhang, Durability of ultra-high performance concrete – A review, Constr Build Mater. 255 (2020) 119296. https://doi.org/10.1016/j.conbuildmat.2020.119296.

[18] N.M. Azmee, N. Shafiq, Ultra-high performance concrete: From fundamental to applications, Case Studies in Construction Materials. 9 (2018) e00197. https://doi.org/10.1016/j.cscm.2018.e00197.

[19] C.-C. Hung, H.-S. Lee, S.N. Chan, Tension-stiffening effect in steel-reinforced UHPC composites: Constitutive model and effects of steel fibers, loading patterns, and rebar sizes, Compos B Eng. 158 (2019) 269–278. https://doi.org/10.1016/j.compositesb.2018.09.091.

[20] J. Luo, X. Shao, W. Fan, J. Cao, S. Deng, Flexural cracking behavior and crack width predictions of composite (steel + UHPC) lightweight deck system, Eng Struct. 194 (2019) 120–137. https://doi.org/10.1016/j.engstruct.2019.05.018.

[21] N.M. Azmee, N. Shafiq, Ultra-high performance concrete: From fundamental to applications, Case Studies in Construction Materials. 9 (2018) e00197. https://doi.org/10.1016/J.CSCM.2018.E00197.

[22] S. Al-Obaidi, M. Davolio, F. Lo Monte, F. Costanzi, M. Luchini, P. Bamonte, L. Ferrara, Structural validation of geothermal water basins constructed with durability enhanced ultra high performance fiber reinforced concrete (Ultra High Durability Concrete), Case Studies in Construction Materials. 17 (2022) e01202. https://doi.org/10.1016/J.CSCM.2022.E01202.

[23] M.C. Caruso, C. Pascale, E. Camacho, L. Ferrara, Comparative environmental and social life cycle assessments of off-shore aquaculture rafts made in ultra-high performance concrete (UHPC), International Journal of Life Cycle Assessment. 27 (2022) 281–300. https://doi.org/10.1007/s11367-021-02017-6.

[24] N. Kannikachalam, D. di Summa, R.P. Borg, E. Cuenca, M. Parpanesi, N. De Belie, L. Ferrara, Assessment of Sustainability and Self-Healing Performances of Recycled Ultra-High-Performance Concrete, ACI Mater J. 120 (2023). https://doi.org/10.14359/51737336.

[25] Y. Shao, A. Parks, C.P. Ostertag, Carbon Footprint between Steel-Reinforced Concrete and UHPC Beams, Journal of Structural Engineering. 149 (2023). https://doi.org/10.1061/JSENDH.STENG-11449.

[26] M. Parpanesi, A holistic life-cycle design approach to structures with advanced cement based materials, Politecnico di Milano, 2021.

[27] Caterpillar products, (2019). https://www.cat.com/en_US/products/new/equipment/excavators/large-excavators/104201.html (accessed February 7, 2023).

[28] Cen, EN 1990:2002, Eurocode - Basis of structural design, (2002).

[29] Cen, UNI EN 206:2016, Concrete - Specification, performance, production and conformity, (2016).

[30] E. Cuenca, M. Criado, M. Giménez, M.C. Alonso, L. Ferrara, Effects of Alumina Nanofibers and Cellulose Nanocrystals on Durability and Self-Healing Capacity of Ultrahigh-Performance Fiber-Reinforced Concretes, Journal of Materials in Civil Engineering. 34 (2022). https://doi.org/10.1061/(ASCE)MT.1943-5533.0004375.

[31] J. Fládr, P. Bílý, Specimen size effect on compressive and flexural strength of high-strength fibre-reinforced concrete containing coarse aggregate, Compos B Eng. 138 (2018) 77–86. https://doi.org/10.1016/J.COMPOSITESB.2017.11.032.

[32] S. Al-Obaidi, S. Dicembre, M. Davolio, M. Del Galdo, F. Lo Monte, L. Ferrara, Flexural performance of Ultra High Performance Concrete slabs under simultaneous environmental and mechanical loading, in: Fib Symposium, 2022: pp. 113–120.

[33] S. Timoshenko, S. Woinowsky-Krieger, Theory of Plates and Shells, Engineerin, 1959.

[34] F. Lo Monte, L. Ferrara, Tensile behaviour identification in Ultra-High Performance Fibre Reinforced Cementitious Composites: indirect tension tests and back analysis of flexural test results, Mater Struct. 53 (2020) 145. https://doi.org/10.1617/s11527-020-01576-8.

[35] fib, fib Model Code for Concrete Structures 2010, Wiley-VCH Verlag GmbH & Co. KGaA, Weinheim, Germany, 2013. https://doi.org/10.1002/9783433604090.

[36] Cen, EN 1992-2:2005, Eurocode 2 - Design of concrete structures - Concrete bridges - Design and detailing rules, (2005).

[37] F. du béton and J.C. Walraven, Model Code 2010: Volume 1. Bulletin (fib Fédération internationale du béton).International Federation for Structural Concrete (fib)., 2012.

[38] V.G. Papadakis, C.G. Vayenas, M.N. Fardis, Physical and chemical characteristics affecting the durability of concrete, ACI Mater J. 88 (1991) 186–196.

[39] M.C. Alonso, M. Sanchez, Analysis of the variability of chloride threshold values in the literature, Materials and Corrosion. 60 (2009) 631–637. https://doi.org/10.1002/maco.200905296.

[40] D. di Summa, M. Parpanesi, N. De Belie, L. Ferrara, How to address sustainability and economic viability of advanced cementitious based materials by means of Life Cycle Assessment (LCA) and Life Cycle Cost (LCC) tools integrated into a holistic design-wise approach., in: ICSHM2022 Milano -8thInternational Conference on Self-Healing Materials, 2022: p. 105.

[41] M. Shafikhani, S.E. Chidiac, Quantification of concrete chloride diffusion coefficient – A critical review, Cem Concr Compos. 99 (2019) 225–250. https://doi.org/10.1016/j.cemconcomp.2019.03.011.

[42] A.A. Torres-Acosta, F.J. Presuel-Moreno, C. Andrade, Electrical resistivity as durability index for concrete structures, ACI Mater J. 116 (2019) 245–253. https://doi.org/10.14359/51718057.

[43] Y. Liu, F.J. Presuel-Moreno, M.A. Paredes, Determination of chloride diffusion coefficients in concrete by electrical resistivity method, ACI Mater J. 112 (2015) 631–640. https://doi.org/10.14359/51687777.

[44] BFUHP Bétons Fibrés à Ultra Hautes Performances, (n.d.). http://www.bfuhp.fr/ (accessed July 27, 2022).

[45] E. Cuenca, M. Criado, M. Giménez, M.C. Alonso, L. Ferrara, Effects of Alumina Nanofibers and Cellulose Nanocrystals on Durability and Self-Healing Capacity of Ultrahigh-Performance Fiber-Reinforced Concretes, Journal of Materials in Civil Engineering. 34 (2022). https://doi.org/10.1061/(ASCE)MT.1943-5533.0004375.

[46] B. Van Belleghem, Effect of Capsule-Based Self-Healing on Chloride Induced Corrosion of Reinforced Concrete, PhD Thesis. Ghent University, Belgium, 2018.

[47] D. V. Val, R.E. Melchers, Reliability of Deteriorating RC Slab Bridges, Journal of Structural Engineering. 123 (1997) 1638–1644. https://doi.org/10.1061/(ASCE)0733-9445(1997)123:12(1638).

[48] J. Harnisch, M. Raupach, The residual cross section factor as a key parameter for the static evaluation of corroding reinforced concrete structures, Materials and Corrosion. 66 (2015) 829–838. https://doi.org/10.1002/maco.201408066.

[49] S.U. Balouch, J.P. Forth, J.-L. Granju, Surface corrosion of steel fibre reinforced concrete, Cem Concr Res. 40 (2010) 410–414. https://doi.org/10.1016/j.cemconres.2009.10.001.

[50] S. Alobaidi, S. He, E. Schlangen, L. Ferrara, Effect of matrix Self-Healing on the Bond-Slip Behavior of Micro Steel Fibers in Ultra High-Performance Concrete, (2023). https://doi.org/10.21203/rs.3.rs-2841443/v1.

[51] J.-L. Granju, S.U. Balouch, Corrosion of steel fibre reinforced concrete from the cracks, Cem Concr Res. 35 (2005) 572–577. https://doi.org/10.1016/j.cemconres.2004.06.032.

[52] G. Naidu Gopu, S.A. Joseph, Corrosion Behavior of Fiber-Reinforced Concrete—A Review, Fibers. 10 (2022) 38. https://doi.org/10.3390/fib10050038.

[53] J.O. Rivera-Corral, G. Fajardo, G. Arliguie, R. Orozco-Cruz, F. Deby, P. Valdez, Corrosion behavior of steel reinforcement bars embedded in concrete exposed to chlorides: Effect of surface finish, Constr Build Mater. 147 (2017) 815–826. https://doi.org/10.1016/j.conbuildmat.2017.04.186.

[54] D. Jia, Q. Guo, J. Mao, J. Lv, Z. Yang, Durability of glass fibre-reinforced polymer (GFRP) bars embedded in concrete under various environments. I: Experiments and analysis, Compos Struct. 234 (2020). https://doi.org/10.1016/j.compstruct.2019.111687.

[55] C. Fu, K. Zhou, Y. Ling, X. Jin, D. Fang, J. Zhou, Chloride transport behavior in bending-shear section of reinforced concrete beam under combined effect of load and environment, Constr Build Mater. 257 (2020). https://doi.org/10.1016/j.conbuildmat.2020.119533.

[56] Y. Murad, A. Tarawneh, F. Arar, A. Al-Zu'bi, A. Al-Ghwairi, A. Al-Jaafreh, M. Tarawneh, Flexural strength prediction for concrete beams reinforced with FRP bars using gene expression programming, Structures. 33 (2021) 3163–3172. https://doi.org/10.1016/j.istruc.2021.06.045.

[57] A. Bossio, G.P. Lignola, F. Fabbrocino, T. Monetta, A. Prota, F. Bellucci, G. Manfredi, Nondestructive assessment of corrosion of reinforcing bars through surface concrete cracks, Structural Concrete. 18 (2017) 104–117. https://doi.org/10.1002/suco.201600034.

[58] X. Zhang, Y. Zhang, B. Liu, B. Liu, W. Wu, C. Yang, Corrosion-induced spalling of concrete cover and its effects on shear strength of RC beams, Eng Fail Anal. 127 (2021) 105538. https://doi.org/10.1016/j.engfailanal.2021.105538.

[59] CEN, EN 1995-1-1:2004 Eurocode 5: Design of timber structures - Part 1-1: General - Common rules and rules for buildings, (2004).

[60] E. Cuenca, F. Lo Monte, M. Moro, A. Schiona, L. Ferrara, Effects of Autogenous and Stimulated Self-Healing on Durability and Mechanical Performance of UHPFRC: Validation of Tailored Test Method through Multi-Performance Healing-Induced Recovery Indices, Sustainability. 13 (2021) 11386. https://doi.org/10.3390/su132011386.

[61] L. Ferrara, V. Krelani, F. Moretti, Autogenous healing on the recovery of mechanical performance of High Performance Fibre Reinforced Cementitious Composites (HPFRCCs): Part 2 e Correlation between healing of mechanical performance and crack sealing, Cem Concr Compos. 73 (2016) 299–315. https://doi.org/10.1016/j.cemconcomp.2016.08.003.

[62] M. Davolio, S. Al-Obaidi, M.Y. Altomare, F. Lo Monte, L. Ferrara, A methodology to assess the evolution of mechanical performance of UHPC as affected by autogenous healing under sustained loadings and aggressive

exposure conditions, Cem Concr Compos. 139 (2023) 105058. https://doi.org/10.1016/J.CEMCONCOMP.2023.105058.

[63] J.Á. López, P. Serna, J. Navarro-Gregori, H. Coll, A simplified five-point inverse analysis method to determine the tensile properties of UHPFRC from unnotched four-point bending tests, Compos B Eng. 91 (2016) 189–204. https://doi.org/10.1016/j.compositesb.2016.01.026.

[64] A. Cibelli, G. Di Luzio, L. Ferrara, Numerical modelling via a coupled discrete approach of the autogenous healing for Fibre-Reinforced Cementitious Composites (FRCCs), in: Computational Modelling of Concrete and Concrete Structures, CRC Press, London, 2022: pp. 86–95. https://doi.org/10.1201/9781003316404-10.

[65] UNI, UNI EN ISO 14040:2021, Environmental management - Life cycle assessment - Principles and framework, (2021).

[66] UNI, UNI EN ISO 14044:2021, Environmental management - Life cycle assessment - Requirements and guidelines, (2021).

[67] UNI, UNI EN 15804:2019, Sustainability of construction works - Environmental product declarations - Core rules for the product category of construction products, (2019).

[68] European FEICA - Association of the, A. and S. Industry, ENVIRONMENTAL PRODUCT DECLARATION as per ISO 14025 and EN 15804. Dispersion-based products, 2016.

[69] A. de Souza Oliveira, O. da Fonseca Martins Gomes, L. Ferrara, E. de Moraes Rego Fairbairn, R.D. Toledo Filho, An overview of a twofold effect of crystalline admixtures in cement-based materials: from permeability-reducers to self-healing stimulators, Journal of Building Engineering. 41 (2021) 102400. https://doi.org/10.1016/j.jobe.2021.102400.

[70] European Commission, EU Construction & Demolition Waste Management Protocol, 2016. https://single-market-economy.ec.europa.eu/news/eu-construction-and-demolition-waste-protocol-2018-09-18_en (accessed July 19, 2023).

[71] C.D.M. Emilia-Romagna, Provveditorato interregionale alle Opere Pubbliche di Lombardia ed, PREZZARIO REGIONALE delle opere pubbliche, (2019).

[72] Regione Toscana, Prezzario dei Lavori della Toscana 2021 - Provincia di Siena. Prezzario, Regione Toscana, (2021).

[73] M.C. Caruso, C. Pascale, E. Camacho, S. Scalari, F. Animato, M.C. Alonso, M. Gimenez, L. Ferrara, Life cycle assessment on the use of ultra high performance fibre reinforced concretes with enhanced durability for structures in extremely aggressive environments: Case study analyses, 2020. https://doi.org/10.1007/978-3-030-43332-1_24.

[74] V. Cappellesso, D. di Summa, P. Pourhaji, N. Prabhu Kannikachalam, K. Dabral, L. Ferrara, M.C. Alonso, E. Camacho, E. Gruyaert, N. De Belie, A review of the efficiency of self-healing concrete technologies for durable and sustainable concrete under realistic conditions, Submitted to International Materials Reviews. (2022).

[75] M.C. Caruso, M. Luchini, S. Montomoli, E. Camacho, E. Nteze, S. Sideri, E. Gastaldo, A. Tretjakov, Reshealience D7.1 - Life Cycle Sustainability Assessment: LCA LCC and SLCA, 2020.

[76] D. di Summa, M. Parpanesi, L. Ferrara, N. De Belie, Life Cycle Assessment (LCA) and Life Cycle Cost (LCC) analysis as crucial part of a holistic approach to the design of structures with advanced cement based materials, in: 76th RILEM Annual Week and International Conference on Regeneration and Conservation of Structures (ICRCS 2022), 2022.